Data Science Enables Chemical Interpretation of HBC-Catalyzed Polymerization for Poly(disulfide)s

Miaomiao Zhang,‡ Yuming Su,‡ Tianyi Du, Jieyu Dai, Cheng Wang*, Yun Liu*

Abstract

H-Bonding catalysts (HBCs) has gained widespread success in improving the selectivity of organic synthesis. The complexity of potentially engaging noncovalent interactions have imposed significant challenges in deciphering the contributing factors of these catalytic reactions. Herein, we present the use of interpretable machine learning on HBCs applied in poly(disulfide) synthesis, wherein the epiquinine-derived thiourea HBCs enable simultaneous regioselectivity control and rate acceleration over the otherwise unselective and already rapid polymerization. A training set of 28 catalysts with variation on the phenyl substituents were synthesized and tested to gather experimental observables: the apparent rate (k_p) and regioselectivity (P_{ss}). Considering the limited data size, we applied the feature-sensitive XGBoost algorithm for supervised machine learning. Upon screening over 64 potentially relevant descriptors, a reasonable fitting of the observables was established for k_p ($R^2 = 0.76$) and P_{ss} ($R^2 = 0.91$), and the key catalyst features necessary for achieving high reaction rates and regioselectivity were deconvoluted. The model suggests that sterically hindered, heavy atom-containing substituents or strongly electro-withdrawing groups on the HBC adversely affect the reaction rate. Substituents enhancing the electrostatic potential of the aromatic N atom are beneficial for achieving high regioregularity, while presence of *ortho*-substituents on the phenyl ring is unfavorable.

INTRODUCTION

The general use of small organic molecules as catalysts for organic synthesis has been known for more than a century already, but the rise of the concept of "organic catalysis" in this field is mainly attributed to the works published by List and McMillan in 2000[1-4]. Until 2021, asymmetric organic catalysis was developed as a new and precise molecular construction tool, for which they were awarded the Nobel Prize in Chemistry. Organic catalysis provides many advantages for the synthesis of organic chemistry. Compared to many transition metal catalysts, they are stable to air and water, easy to treatment, relatively non-toxic, and easy to separate from crude reaction mixtures. Moreover, organic catalysts are easily obtained from natural sources or prepared in a few simple steps. Currently, small organic molecule catalysts are widely used, including chiral ketones[5-7], urea/thiourea[8-11], proline and its derivatives[12-14], DMAP derivatives[15,16], chiral phosphoramides[17-20], quaternary ammonium salts[21,22], etc. Some fundamental activation and catalysis modes like enamine and iminium activation, Brønsted acid/base catalysis, nucleophilic Lewis base catalysis, H-bonding catalysis, and quaternary (amm)onium salt ion pairing phase-transfer catalysis belong to the established and most commonly used catalysis concepts in the realm of asymmetric organocatalysis[23]. Organocatalysts that function via hydrogen bonding has been developed, particularly urea/thiourea. They having two H-bonding NH's, have found extensive application in organocatalyzed reactions[10,24-30].

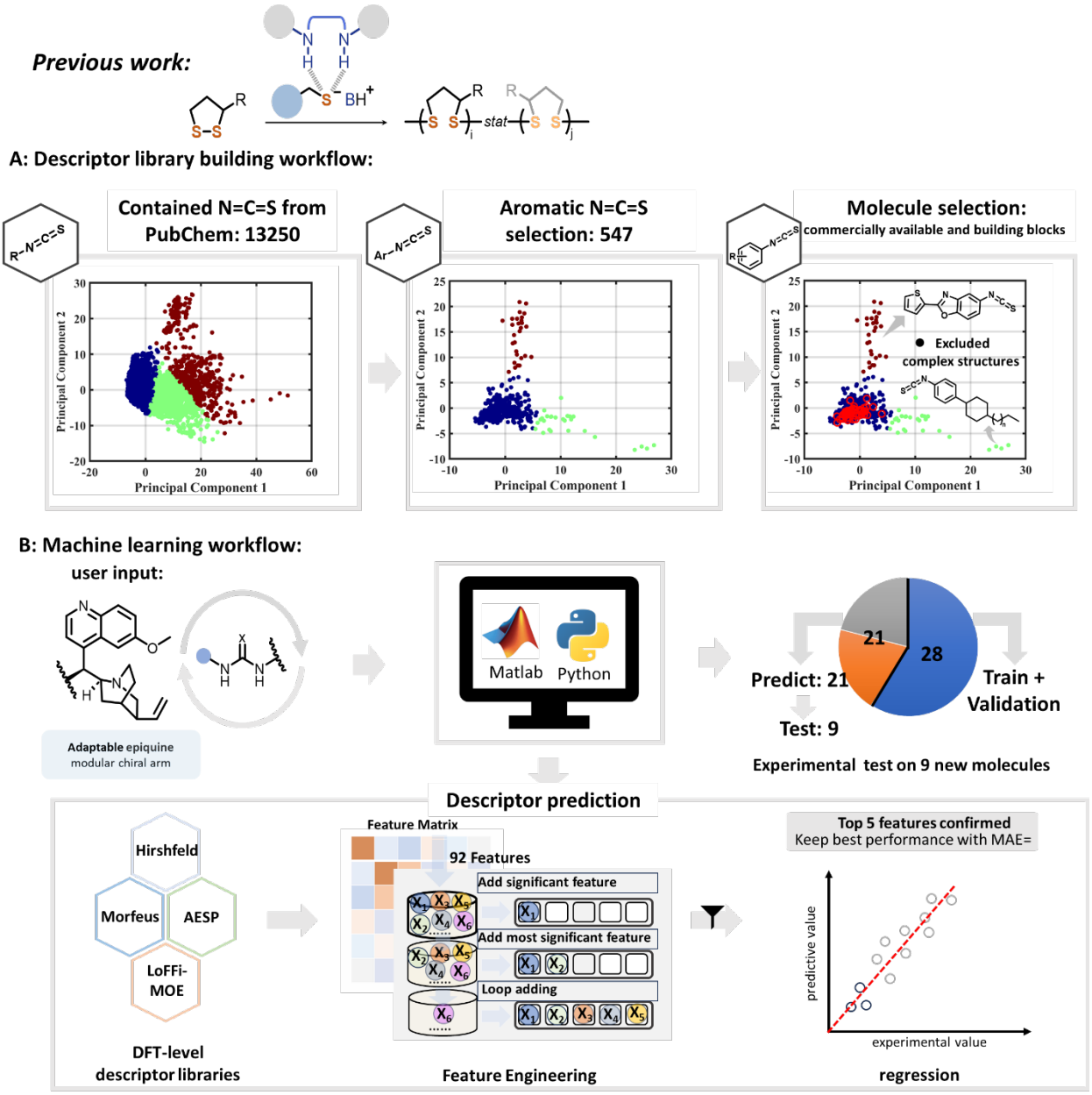

Figure 1. ML workflow for the ROP of 1,2-dithiolanes, targeting enhanced polymerization rate and regioselectivity with an initial set of catalysts.

Furthermore, among the various catalysts for ring-opening polymerization (ROP), H-bonding organocatalysts stand out in the precise and controllable ways of the synthesized polymers[31-35]. This class of catalyst is constituted by one of a host of H-bond donating moieties

(most commonly thiourea or urea) and a base cocatalyst[36]. For example, the synthesis of polyphosphoesters, aliphatic polyesters and polycarbonates were accomplished by addition of thiourea catalyst and base to catalyze ring-opening by Waymouth and Hedrick[37]. The H-bonding class of organocatalysts are thought to effect ROP via dual activation of both monomer and chain end. It is generally believed that there are two activation mechanisms: one is the neutral hydrogen bonding mechanism, another is the mechanism mediated by imidate or thioimidate species. The operative mechanism depends most greatly on the solvent, where polar solvents favor an imidate/thioimidate mechanism and nonpolar solvents favor a classic H-bond mediated ROP[38,39]. And the models mentioned above has been widely verified with ^{1}H NMR titration experiments. Actually, it can be difficult because of the complicated and sensitive interplay of interactions that give rise to catalysis. H-bonding catalysts are known to bind to monomer, base, each other and other species to a lesser extent (i.e., polymer). Furthermore, DFT calculation data in mechanism research suggest that the transition state is only modeled with ground state thiourea−monomer interactions in the H-bonding pathway. It is just the complexity of interactions and species changes during the reaction process that limited the explanation of reaction mechanism. To address this challenge, our investigated perspective article summarizes current computational approaches used in molecular catalyst design, highlights their main advantages and limitations as well as the opportunities for automation and advanced machine learning algorithms[40,41].

Previously, we developed an anion-binding approach to arrest the high reactivity of RS^{-} chain end to control the dynamic covalent synthesis of linear poly(disulfide)s. Derived Cinchona

thiourea catalyst and TMG/BnSH achieve a rapid, living ring-opening polymerization of 1,2-dithiolanes with narrow dispersity and high regioregularity ($M_w/M_n \sim 1.1$, $P_{ss} \sim 0.8$)[42]. The key catalyst features necessary for achieving narrow dispersity and high regioregularity were unseen, computational methods have emerged as a powerful tool to augment traditional experimental molecular catalyst design by providing useful predictions of catalyst performance and decreasing the time needed for catalyst screening.

In this study, we demonstrate a 3-round machine learning (ML) approach that critically informs the reaction optimization and mechanistic interrogation of hydrogen bonding catalysis in the ring-opening polymerization of 1,2-dithiolanes. In the second round of ML, we distilled interpretable conclusions and generated a list of catalyst recommendations from a commercially available database. Subsequent experimental validation in the third round confirmed that while most catalysts aligned with ML predictions, they exhibited moderate performance. However, it was an outlier—an unforeseen catalyst not predicted by our model—that achieved an exceptional polymerization rate. This serendipitous discovery highlights both the power and current limitations of ML in catalysis research. The high-performing catalyst identified defies the explanatory power of our existing ML framework, underscoring the need for ongoing refinement of our predictive models. This catalyst, which emerged from the data-driven discovery pipeline, underscores the nuanced interplay between empirical experimentation and algorithmic prediction, marking a significant step forward in the rational design and data-augmented exploration of advanced catalytic materials.

RESULTS AND DISCUSSION

Training set design and synthesis. A major work is that we selected an assortment of commercially available aromatic isothiocyanates from monosubstituted to trisubstituted or synthesized through simple one or two steps for the catalyst library. Deriving 28 thiourea catalysts from quinine to ensure a spread of polymerization data as required for effective statistical modeling (**Figure 2**). To efficiently assess this unique catalyst scaffold both computationally and experimentally, we aimed to develop a workflow to identify key catalyst features and present further evidence that scaffold optimization should be considered in future catalyst designs. We also expect to eventually provide meaningful mechanistic insights into the origin of selectivity for the reaction under study.

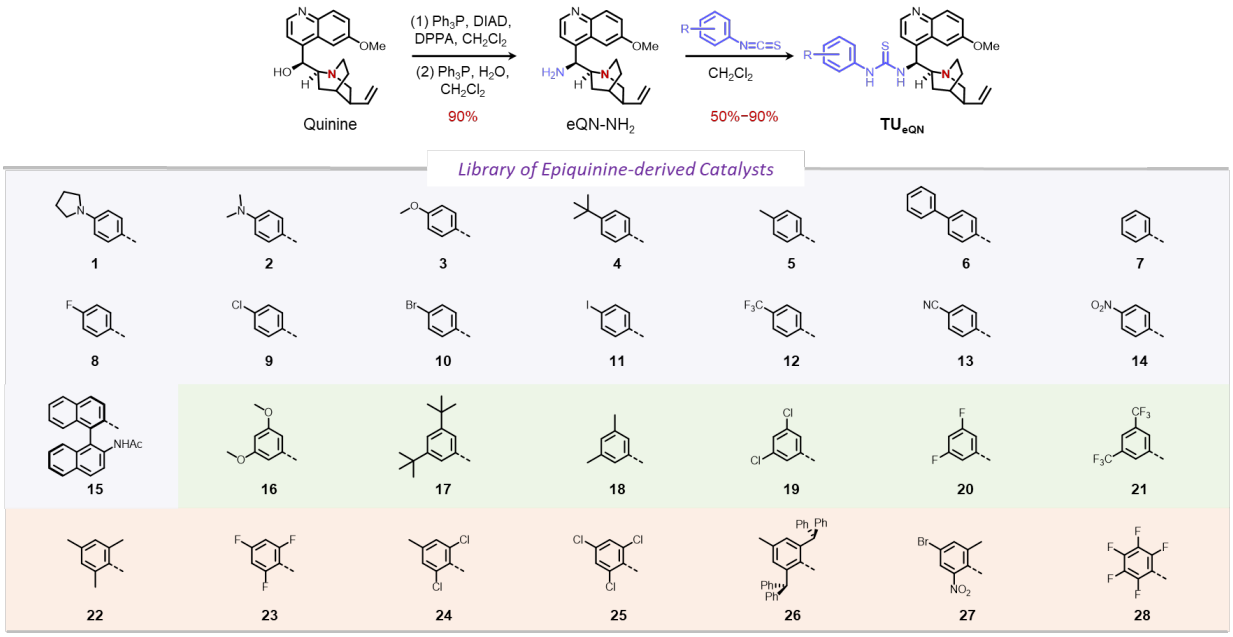

Figure 2. Synthetic route to access training set of Epiquinine-derived catalyst candidates.

We chose the reported ring-opening polymerization of 1,2-dithiolanes, and screened all the catalysts of the established catalyst library under standard polymerization conditions. Experiments show that a series of catalysts derived from quinine can achieve controlled living polymerization of **R-LpMe (see in SI)**, and the small-scale editing of the catalyst skeleton can regulate the polymerization rate and the regioselectivity of the polymerization reaction. The polymerization results show (**Figure 3**) that the 4-position substituent of the aromatic ring in the fragment derived from the aromatic isothiocyanate in the catalyst is changed from electron-donating to electron-withdrawing. The polymerization rate does not show a simple single-variable linear relationship determined by the ability to push and absorb electrons. This finding is also reflected in the catalyst system of di-substituted, tri-substituted and pentafluoro-substituted. To our surprise, when both the polymerization rate and the regioselectivity of the polymerization reaction are considered, the halogenated and quasi-halogenated catalysts show a win-win characteristic except for a few special cases. The polymerization rate and regioselectivity are converted into energy. As shown in the figure, we also focus on the catalyst from trifluoro- **23** to pentafluoro- **28**, which improves the polymerization regioselectivity (P_{ss}: 0.72–0.76) while sacrificing the polymerization rate (k_p: 3.36–0.16 h^{-1}). In view of the above experimental results, we hypothesize that in the ring-opening polymerization system of **R-LpMe**, the catalytic behavior of the catalyst in the polymerization is a result of multiple factors.

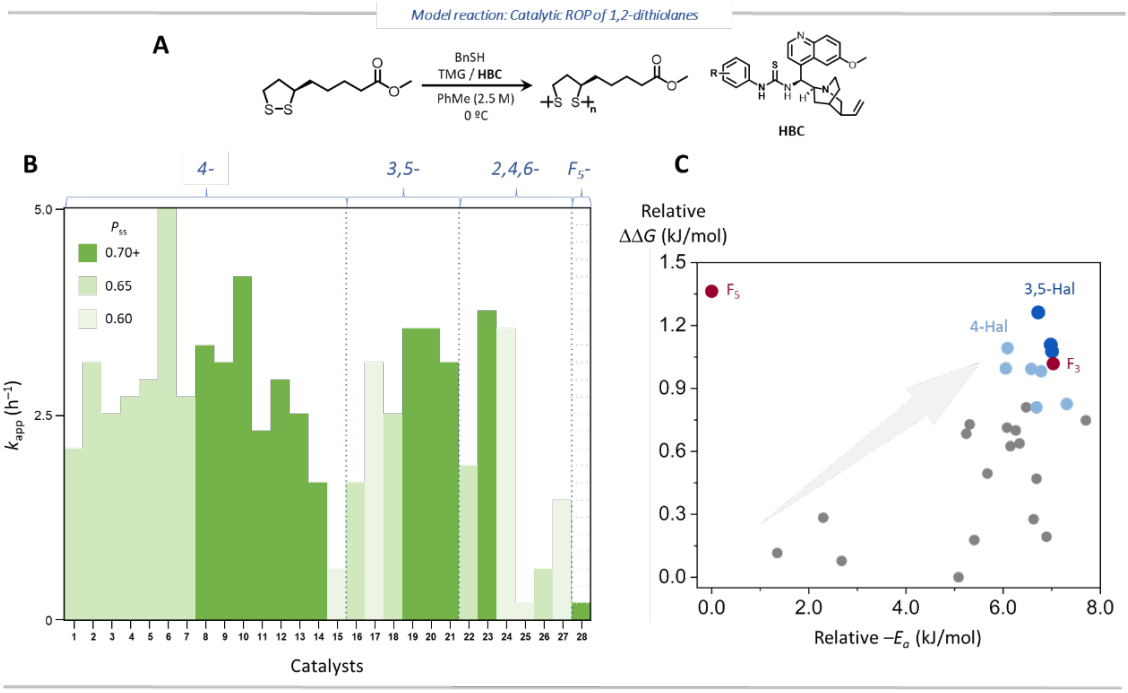

Figure 3. Polymerization screen using 28 reported organocatalysts above. (A) Model reaction platform used to study the kinetics and regioselectivity of polymerization. (B) Histogram represent reaction rate (k_{app}) and regioselectivity (P_{ss}) shown by each catalyst. (C) Energy distribution diagram conversed by k_{app} and P_{ss}.

Machine Learning by the Tree-Based XGBoost Algorithm. In our initial phase, we adopted Morfeus and Hirshfeld charge as features and employed multivariate linear regression models for machine learning. The outcomes for polymerization rate objectives were nonideal, with a mean absolute error (MAE) of 0.792 and an R^2 value of 0.184, indicating a poor predictive performance (**Figure 4B** and **4C**). However, the model showed a slightly better performance in predicting polymerization regioselectivity, which prompted us to further investigate and develop new descriptors to enhance our understanding and prediction accuracy.

Leveraging the capabilities of Multiwfn, we have developed a method for dissecting the molecular space into distinct atomic regions, named Atomic Electrostatic Potential (AESP) descriptors. The molecular van der Waals surface is partitioned into areas attributed to individual atoms or groups of atoms. By computing electrostatic potential-related statistical metrics on these localized atomic Van der Waals surfaces, our method allows for improved description of atom-specific information crucial for catalytic function. Then we can extract detailed values such as the minimal and maximal electrostatic potential present on the local van der Waals surface of each atom, providing a robust set of atomic electrostatic potential descriptors.

In the 2nd gen of our machine learning initiative, we expanded upon the initial descriptor framework by incorporating atomic electrostatic potential descriptors and conjugation descriptors, the latter of which were proposed in our prior work on characterizing the two-photon absorption properties of organic molecules. For this phase, we employed the XGBoost model along with stepwise regression for feature selection. By randomly splitting the dataset 160 times, we ascertained each molecule's average error and prediction standard deviation within the test sets, ensuring the robustness of our models. Remarkably, this procedure effectively reduced the number of features from 94 to 5, while a significant improvement in the model's predictive capability for both k_p and P_{ss} was established. As shown in Figure 4 (e) and (f), for the k_p target, the MAE was reduced to 0.426 and the R^2 increased to 0.755. For P_{ss}, the MAE decreased to 0.0098 and the R^2 reached an impressive 0.907. At this juncture, we consider our model to be well-tuned for the dataset comprising 28 molecules.

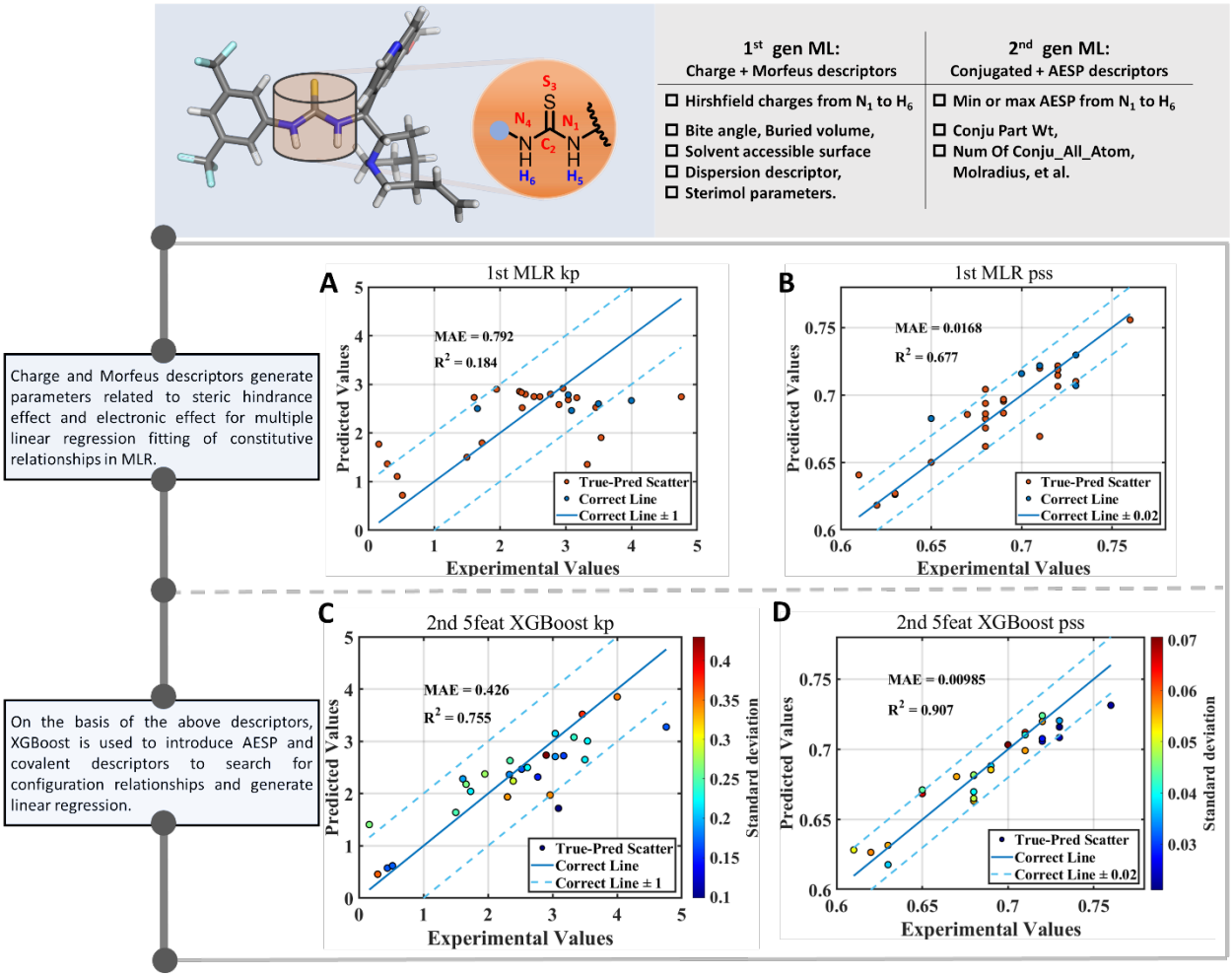

Figure 4. Features and performance metrics for round one and two of machine learning. Mean absolute error (MAE) and coefficient of determination are annotated.

Interpretation of Contributing Structural Features. Furthermore, we leveraged SHAP (SHapley Additive exPlanations) analysis, a game theory-based approach, to provide individual contributions for each feature of every sample, offering human-interpretable chemical insights. In the analysis of the model, it was found that among the five characteristics related to the polymerization rate, the two most significant features were the deviation of the atomic mass of the largest conjugated part (**Conju_Part_Wt**) and the minimum atomic electrostatic potential

point of **N4ESPmin**. The former captures the steric hindrance effect of the substituent groups; bulky substituents or those with heavier atoms are typically detrimental to the reaction rate. For example, molecules with iodine or bromine substitutions, as well as those with significant steric bulk, can be seen in SHAP analysis plots to have an adverse effect on k_p, sometimes decreasing it to nearly unity. This highlights the effective portrayal of this feature in describing the steric hindrance effect.

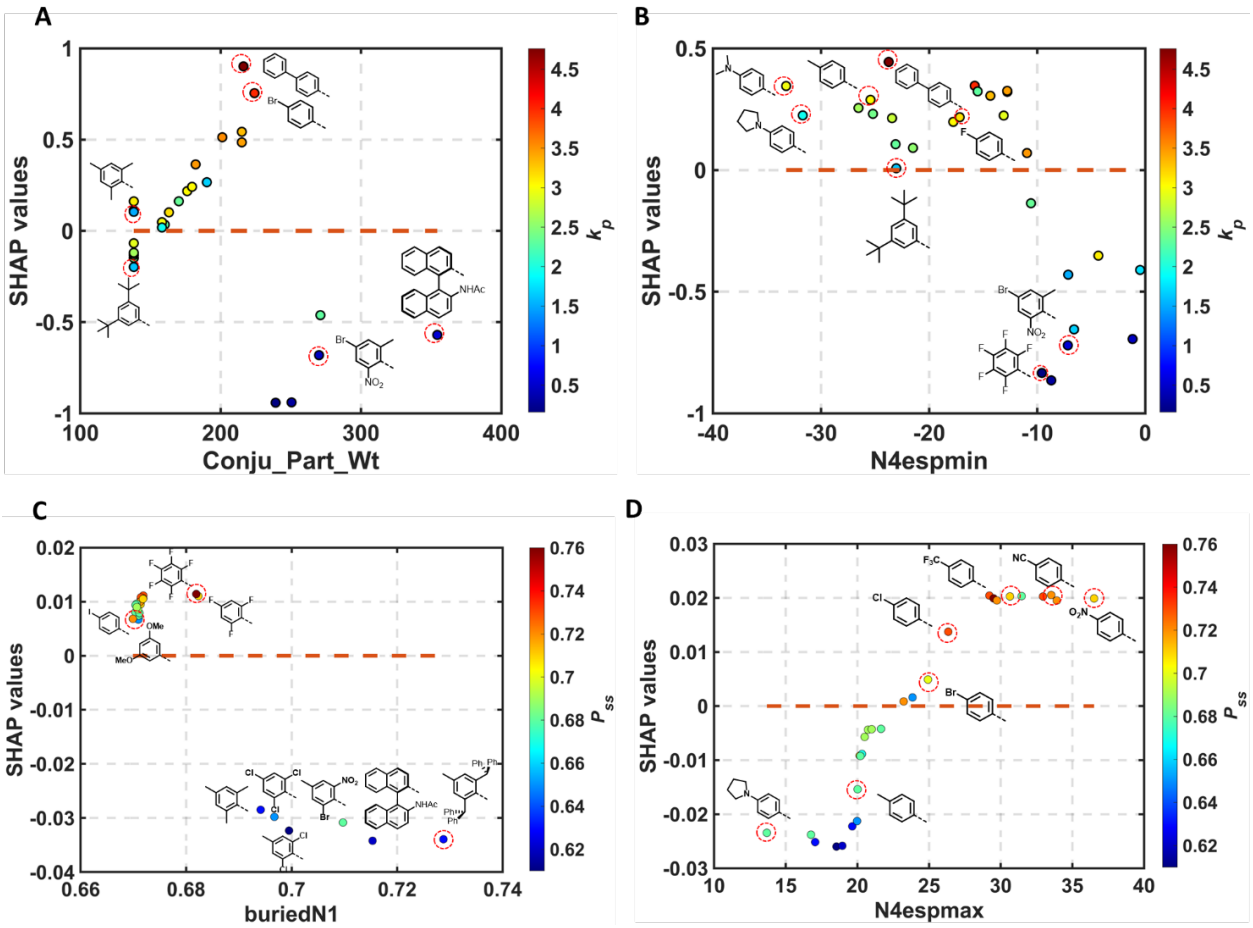

Figure 5. SHAP analysis of (A) **Conju_Part_Wt**, (B) **N4espmin** for k_p, (C) **buriedN1** and (D) **N4espmax** for P_{ss}

On the other hand, some catalysts that are modified might seem at first glance to benefit k_p from increasing conjugated mass. However, this is attributed to the nature of tree-based models like XGBoost, which "categorize" samples. It just so happens that some of the heavier molecules also have large steric hindrances or other factors that are unfavorable for k_p. The latter feature, **N4ESPmin**, reflects the structural capability of the catalyst molecule to be polarized. The presence of substituents can lead to either too little or too much uneven charge distribution on the molecule's surface area, which can be unfavorable for the reaction rate. **N4ESPmin**, effectively characterizes the molecule's electron-donating or -withdrawing properties, organizing modifications like amino, pyrrole, and nitro groups in a manner that allows XGBoost to better quantify their electron-donating or -withdrawing characteristics. according to SHAP analysis plots, can influence the polymerization rate to varying degrees, ranging from a decrease of up to -1 to an increase of 0.5. Two of the five characteristics closely related to the regioselectivity are: the embedding volume of the N of the NH near the bridge ring (**buriedN1**) and the maximum electrostatic potential on the surface of the N of the bridge ring (**N4espmax**). The former is the embodiment of the steric effect of the substituent, especially the steric of the 2,6-position of the benzene substituent, which is not conducive to P_{ss}. As shown in the figure, from the steric effect of the substituents introduced at the 2,6 positions of the catalyst editable aromatic ring, it can be seen that the steric effect of the introduced substituents gradually increases from catalyst **10** to **22**, and then to **27**, **26**, affecting the embedding volume of the N atom near the bridge ring NH′s, showing a change in the direction unfavorable to the polymerization region selectivity (P_{ss}). The latter is the embodiment of the

electronic effect of the substituent. The larger the surface electrostatic potential of the bridge ring N atom, the more electropositive it shows, the more electrophilic it is, and the easier it is to react with S^- intrinsically, the larger the more favorable the P_{ss}. These features can be shown from the SHAP scatter plot following (**Figure 5C**), catalyst **1** with strong electron-donating substituent to catalysts **10**, **14** and **19** with electron-withdrawing substituent shows a more favorable trend for P_{ss}. The structure–activity relationships shown above are all understandable. H-Bonding mediated processes take advantage of intrinsic steric and electronic substrate bias to influence the site of nucleophilic attack. Catalyst-controlled steric effect and nucleophilicity by H-Bonding with chain end, which not only regulates the regioselectivity, but also affects the polymerization kinetics[43].

CONCLUSION

In summary, we implemented XGBoost to optimize and understand hydrogen bonding catalysis for the ring-opening polymerization of 1,2-dithiolanes. SHAP analysis based on the supervised machine learning have provided an interpretative framework for both the reaction rate and regioselectivity. The influence of electronic effect of the substituents was shown to follow opposite trend between reaction rates and regioselectivity, explaining the experimental observation that halogenated HBCs have the overall best performance. The size of the substituents also needs to be balanced so that a necessary steric hindrance is imposed on the catalytic pocket without sacrificing the rate. Thus, the *meta*-position was revealed to be ideal for placing substituents. The design and synthesis of new HBC based on these insights are currently ongoing.

ASSOCIATED CONTENT

Supporting Information

Experimental and computational procedures, synthesis and characterization of new compounds, GPC and NMR data for polymerization of different conditions, theoretical analysis of regioregularity, computational results, and XYZ coordinates (PDF)

AUTHOR INFORMATION

Corresponding Author

Cheng Wang − *Collaborative Innovation Center of Chemistry for Energy Materials, State Key Laboratory of Physical Chemistry of Solid Surfaces, Department of Chemistry, College of Chemistry and Chemical Engineering, Xiamen University, Xiamen 361005, P. R. China*; ORCID: 0000-0002-7906-8061; Email: wangchengxmu@xmu.edu.cn

Yun Liu − *Beijing National Laboratory for Molecular Sciences, Center for Soft Matter Science and Engineering, Key Laboratory of Polymer Chemistry and Physics of Ministry of Education, College of Chemistry and Molecular Engineering, Peking University, Beijing 100871, China*; ORCID: 0000-0001-7077-363X; Email: yun.liu@pku.edu.cn

Authors

Miaomiao Zhang − *Beijing National Laboratory for Molecular Sciences, Center for Soft Matter Science and Engineering, Key Laboratory of Polymer Chemistry and Physics of Ministry of Education, College of Chemistry and Molecular Engineering, Peking University, Beijing 100871, China*

Yuming Su − *State Key Laboratory of Physical Chemistry of Solid Surfaces, Department of Chemistry, College of Chemistry and Chemical Engineering, iChem, Innovation Laboratory for Sciences and Technologies of Energy Materials of Fujian Province (IKKEM), Xiamen University, 361005 Xiamen, P. R. China*

Tianyi Du − *Beijing National Laboratory for Molecular Sciences, Center for Soft Matter Science and Engineering, Key Laboratory of Polymer Chemistry and Physics of Ministry of Education, College of Chemistry and Molecular Engineering, Peking University, Beijing 100871, China*

Jieyu Dai − *Beijing National Laboratory for Molecular Sciences, Center for Soft Matter Science and Engineering, Key Laboratory of Polymer Chemistry and Physics of Ministry of Education, College of Chemistry and Molecular Engineering, Peking University, Beijing 100871, China*

Author Contributions

§M.Z. and Y.S. contributed equally.

Notes

The authors declare no competing financial interest.

ACKNOWLEDGMENTS

This work was supported by the National Natural Science Foundation of China (22271005), the Beijing National Laboratory for Molecular Sciences. Y.S. and C.W. acknowledge the financial

support from the Fundamental Research Funds for the Central Universities (No. 20720220011).

We thank Beijing NMR Center at Peking University for their assistance in 2D NMR experiments.

REFERENCES

(1) Tehshik P. Yoon, V. M. D., David W. C. MacMillan. Development of a New Lewis Acid-Catalyzed Claisen Rearrangement. *J. Am. Chem. Soc.* **1999**, *121*, 9726-9727.
(2) Wendy S. Jen, J. J. M. W., David W. C. MacMillan. New Strategies for Organic Catalysis: The First Enantioselective Organocatalytic 1,3-Dipolar Cycloaddition. *J. Am. Chem. Soc.* **2000**, *122*, 9874-9875.
(3) Wolfgang Notz, B. L. Catalytic Asymmetric Synthesis of anti-1,2-Diols. *J. Am. Chem. Soc.* **2000**, *122*, 7386-7387.
(4) List, B. The Direct Catalytic Asymmetric Three-Component Mannich Reaction. *J. Am. Chem. Soc.* **2000**, *122*, 9336-9337.
(5) Curran, D. P.; Zhang, Q.; Richard, C.; Lu, H.; Gudipati, V.; Wilcox, C. S. Total Synthesis of a 28-Member Stereoisomer Library of Murisolins. *J. Am. Chem. Soc.* **2006**, *128*, 9561-9573.
(6) Yong Tu, M. F., Zhi-Xian Wang, Yian Shi. Synthesise of 1,2:4,5-Di-O-Isopropylidene-D-erythro-2,3-hexodiulo-2,6-pyranose. A Highly Enantioselective Ketone Catalyst for Epoxidation. *Org. Synth.* **2003**, *80*.
(7) Sang Min Lim, N. H., Andrew G. Myers. A Method for the Preparation of Differentiated trans-1,2-Diol Derivatives with Enantio- and Diastereocontrol. *J. Am. Chem. Soc.* **2009**, *131*, 5763–5765.
(8) Matthew S. Sigman, E. N. J. Schiff Base Catalysts for the Asymmetric Strecker Reaction Identified and Optimized from Parallel Synthetic Libraries. *J. Am. Chem. Soc.* **1998**, *120*, 4901-4902.
(9) Tomotaka Okino, Y. H., Yoshiji Takemoto. Enantioselective Michael Reaction of Malonates to Nitroolefins Catalyzed by Bifunctional Organocatalysts. *J. Am. Chem. Soc.* **2003**, *125*, 12672-12673.
(10) Benedek Vakulya, S. r. V., Antal Csa´mpai, and Tibor Soo´s. Highly Enantioselective Conjugate Addition of Nitromethane to Chalcones Using Bifunctional Cinchona Organocatalysts. *Org. Lett.* **2005**, *7*, 1968-1969.
(11) Jian Wang, H. L., Xinhong Yu,‡ Liansuo Zu, Wei Wang. Chiral Binaphthyl-Derived Amine-Thiourea Organocatalyst-Promoted Asymmetric Morita−Baylis−Hillman Reaction. *Org. Lett.* **2005**, *7*, 4294-4296.
(12) Benjamin List, R. A. L., Carlos F. Barbas III. Proline-Catalyzed Direct Asymmetric Aldol Reactions. *J. Am. Chem. Soc.* **2000**, *122*, 2395-2396.
(13) Coulthard, G.; Erb, W.; Aggarwal, V. K. Stereocontrolled organocatalytic synthesis of prostaglandin PGF2α in seven steps. *Nature* **2012**, *489*, 278-281.

(14) Zhu, S.; Yu, S.; Wang, Y.; Ma, D. Organocatalytic Michael Addition of Aldehydes to Protected 2-Amino-1-Nitroethenes: The Practical Syntheses of Oseltamivir (Tamiflu) and Substituted 3-Aminopyrrolidines. *Angew. Chem. Int. Ed.* **2010**, *49*, 4656-4660.
(15) J. Craig Ruble, H. A. L., Gregory C. Fu. Effective Kinetic Resolution of Secondary Alcohols with a Planar-Chiral Analogue of 4-(Dimethylamino)pyridine. Use of the Fe(C5Ph5) Group in Asymmetric Catalysis. *J. Am. Chem. Soc.* **1997**, *119*, 1492-1493.
(16) Xie, M. S.; Zhang, Y. F.; Shan, M.; Wu, X. X.; Qu, G. R.; Guo, H. M. Chiral DMAP-N-oxides as Acyl Transfer Catalysts: Design, Synthesis, and Application in Asymmetric Steglich Rearrangement. *Angew. Chem. Int. Ed.* **2019**, *58*, 2839-2843.
(17) Scott E. Denmark, S. B. D. W., Xiping Su, Ken-Tsung Wong. Chemistry of Trichlorosilyl Enolates. 1. New Reagents for Catalytic, Asymmetric Aldol Additions. *J. Am. Chem. Soc.* **1996**, *118*, 7404-7405.
(18) Mi Zeng, S.-L. Y. Asymmetric Friedel–Crafts Alkylation of Indoles: The Control of Enantio- and Regioselectivity. *Synlett* **2009**, *9*, 1289–1301.
(19) Mayer, S.; List, B. Asymmetric Counteranion-Directed Catalysis. *Angew. Chem. Int. Ed.* **2006**, *45*, 4193-4195.
(20) Avila, C. M.; Patel, J. S.; Reddi, Y.; Saito, M.; Nelson, H. M.; Shunatona, H. P.; Sigman, M. S.; Sunoj, R. B.; Toste, F. D. Enantioselective Heck-Matsuda Arylations through Chiral Anion Phase-Transfer of Aryl Diazonium Salts. *Angew. Chem. Int. Ed.* **2017**, *56*, 5806-5811.
(21) Takashi Ooi, M. K., Keiji Maruoka. Molecular Design of a C2-Symmetric Chiral Phase-Transfer Catalyst for Practical Asymmetric Synthesis of r-Amino Acids. *J. Am. Chem. Soc.* **1999**, *121*, 6519-6520.
(22) Yasui, M.; Yamada, A.; Tsukano, C.; Hamza, A.; Pápai, I.; Takemoto, Y. Enantioselective Acetalization by Dynamic Kinetic Resolution for the Synthesis of g-Alkoxybutenolides by Thiourea/Quaternary Ammonium Salt Catalysts: Application to Strigolactones. *Angew. Chem. Int. Ed.* **2020**, *59*, 13479-13483.
(23) García Mancheño, O.; Waser, M. Recent Developments and Trends in Asymmetric Organocatalysis. *Eur. J. Org. Chem.* **2022**, *26*.
(24) Steven M. Banik, A. L., Alan M. Hyde, Eric N. Jacobsen. Lewis acid enhancement by hydrogen-bond donors for asymmetric catalysis. *Science* **2017**, *358*, 761–764.
(25) Kun Liu, H.-F. C., Jing Nie, Ke-Yan Dong, Xiao-Juan Li, and Jun-An Ma. Highly Enantioselective Michael Addition of Aromatic Ketones to Nitroolefins Promoted by Chiral Bifunctional Primary Amine-thiourea Catalysts Based on Saccharides. *Org. Lett.* **2007**, *9*, 923-925.
(26) Herrera, R. P.; Sgarzani, V.; Bernardi, L.; Ricci, A. Catalytic Enantioselective Friedel–Crafts Alkylation of Indoles with Nitroalkenes by Using a Simple Thiourea Organocatalyst. *Angew. Chem. Int. Ed.* **2005**, *44*, 6576-6579.
(27) Xianxing Jiang, Y. Z., Albert S. C. Chan, Rui Wang. Highly Enantioselective Synthesis of γ-Nitro Heteroaromatic Ketones in a Doubly Stereocontrolled Manner Catalyzed by Bifunctional Thiourea Catalysts Based on Dehydroabietic Amine: A Doubly Stereocontrolled Approach to Pyrrolidine Carboxylic Acids. *Org. Lett.* **2009**, *11*, 153-156.

(28) Hayama, N.; Kuramoto, R.; Földes, T.; Nishibayashi, K.; Kobayashi, Y.; Pápai, I.; Takemoto, Y. Mechanistic Insight into Asymmetric Hetero-Michael Addition of α,β-Unsaturated Carboxylic Acids Catalyzed by Multifunctional Thioureas. *J. Am. Chem. Soc.* **2018**, *140*, 12216-12225.
(29) Zhu, Z.; Odagi, M.; Zhao, C.; Abboud, K. A.; Kirm, H. U.; Saame, J.; Lõkov, M.; Leito, I.; Seidel, D. Highly Acidic Conjugate-Base-Stabilized Carboxylic Acids Catalyze Enantioselective oxa-Pictet–Spengler Reactions with Ketals. *Angew. Chem. Int. Ed.* **2019**, *59*, 2028-2032.
(30) Mao Lin Li, J. H. Y., Yi Hao Li, Shou Fei Zhu, Qi-Lin Zhou. Highly enantioselective carbene insertion into N–H bonds of aliphatic amines. *Science* **2019**, *366*, 990–994.
(31) Coderre, D. N.; Fastnacht, K. V.; Wright, T. J.; Dharmaratne, N. U.; Kiesewetter, M. K. H-Bonding Organocatalysts for Ring-Opening Polymerization at Elevated Temperatures. *Macromolecules* **2018**, *51*, 10121-10126.
(32) Xu, J.; Wang, X.; Liu, J.; Feng, X.; Gnanou, Y.; Hadjichristidis, N. Ionic H-bonding organocatalysts for the ring-opening polymerization of cyclic esters and cyclic carbonates. *Prog. Polym. Sci.* **2022**, *125*.
(33) Xu, J.; Liu, J.; Li, Z.; Wang, H.; Xu, S.; Guo, T.; Zhu, H.; Wei, F.; Zhu, Y.; Guo, K. Guanidinium as bifunctional organocatalyst for ring-opening polymerizations. *Polymer* **2018**, *154*, 17-26.
(34) Lin, B. W., R. M. Urea Anions: Simple, Fast, and Selective Catalysts for Ring-Opening Polymerizations. *J. Am. Chem. Soc.* **2017**, *139*, 1645-1652.
(35) Lv, W.; Wang, Y.; Li, M.; Wang, X.; Tao, Y. Precision Synthesis of Polypeptides via Living Anionic Ring-Opening Polymerization of N-Carboxyanhydrides by Tri-thiourea Catalysts. *J. Am. Chem. Soc.* **2022**, *144*, 23622-23632.
(36) Zhang, C.-J.; Wu, H.-L.; Li, Y.; Yang, J.-L.; Zhang, X.-H. Precise synthesis of sulfur-containing polymers via cooperative dual organocatalysts with high activity. *Nat. Commun.* **2018**, *9*.
(37) Andrew P. Dove, R. C. P., Bas G. G. Lohmeijer, Robert M. Waymouth, James L. Hedrick,. Thiourea-Based Bifunctional Organocatalysis: Supramolecular Recognition for Living Polymerization. *J. Am. Chem. Soc.* **2005**, *127*, 13798–13799.
(38) Pothupitiya, J. U.; Hewawasam, R. S.; Kiesewetter, M. K. Urea and Thiourea H-Bond Donating Catalysts for Ring-Opening Polymerization: Mechanistic Insights via (Non)linear Free Energy Relationships. *Macromolecules* **2018**, *51*, 3203-3211.
(39) Hewawasam, R. S.; Kalana, U. L. D. I.; Dharmaratne, N. U.; Wright, T. J.; Bannin, T. J.; Kiesewetter, E. T.; Kiesewetter, M. K. Bisurea and Bisthiourea H-Bonding Organocatalysts for Ring-Opening Polymerization: Cues for the Catalyst Design. *Macromolecules* **2019**, *52*, 9232-9237.
(40) Liles, J. P.; Rouget-Virbel, C.; Wahlman, J. L. H.; Rahimoff, R.; Crawford, J. M.; Medlin, A.; O'Connor, V. S.; Li, J.; Roytman, V. A.; Toste, F. D.; Sigman, M. S. Data science enables the development of a new class of chiral phosphoric acid catalysts. *Chem* **2023**, *9*, 1518-1537.
(41) van Dijk, L.; Haas, B. C.; Lim, N.-K.; Clagg, K.; Dotson, J. J.; Treacy, S. M.; Piechowicz, K. A.; Roytman, V. A.; Zhang, H.; Toste, F. D.; Miller, S. J.; Gosselin, F.; Sigman, M. S. Data

Science-Enabled Palladium-Catalyzed Enantioselective Aryl-Carbonylation of Sulfonimidamides. *J. Am. Chem. Soc.* **2023**, *145*, 20959-20967.
(42) Du, T.; Shen, B.; Dai, J.; Zhang, M.; Chen, X.; Yu, P.; Liu, Y. Controlled and Regioselective Ring-Opening Polymerization for Poly(disulfide)s by Anion-Binding Catalysis. *J. Am. Chem. Soc.* **2023**.
(43) Hubbell, A. K.; Coates, G. W. Nucleophilic Transformations of Lewis Acid-Activated Disubstituted Epoxides with Catalyst-Controlled Regioselectivity. *J. Org. Chem.* **2020**, *85*, 13391-13414.